THE ASTROPHYSICAL JOURNAL, 224:417–436, 1978 September 1

THE CHEMICAL COMPOSITION OF GALACTIC AND EXTRAGALACTIC H II REGIONS*

STEVEN A. HAWLEY†
Lick Observatory, Board of Studies in Astronomy and Astrophysics, University of California, Santa Cruz
Received 1977 November 21; accepted 1978 March 9

ABSTRACT

The results of a spectrophotometric survey of 15 galactic H II regions are presented. From the observed line intensities in the spectral region λλ3700–7100, electron densities, temperatures, and abundances of helium, oxygen, nitrogen, sulfur, and neon are computed. The average helium abundance in galactic H II regions agrees with the average helium abundance in galactic planetary nebulae. The oxygen and nitrogen abundances are found to correlate with the distance of the H II regions from the galactic center in much the same manner as has been proposed previously for other galaxies. The magnitude of the oxygen gradient agrees with that found from planetary nebulae and with the metal gradient found from intermediate age stars. The average abundances in this sample agree well with published abundances in the Orion Nebula.

New observations of H II regions in M101 allow the estimate of abundance gradients and a comparison with abundance gradients in the Galaxy. Generally, the magnitudes of the various gradients agree, although there is some evidence for a steeper nitrogen gradient in the Galaxy. The absolute abundances in H II regions in M101 are probably not different from abundances in the galactic H II regions in this sample.

Subject headings: nebulae: abundances — spectrophotometry

I. INTRODUCTION

Observations of extragalactic H II regions have clearly demonstrated that certain important emission-line ratios vary systematically as a function of position in spiral galaxies. Searle (1971) surveyed H II regions in six Sc galaxies and concluded that the integrated spectra of inner-arm nebulae showed weaker [O III]/Hβ and stronger [N II]/[O II] than did the outer-arm nebulae. His interpretation was that there exists an N/O abundance gradient in these galaxies, with N/O increasing toward the nuclei.

Searle's work motivated several other investigations of line intensity gradients across spiral galaxies, including, for example, those of Benvenuti, D'Odorico, and Peimbert (1973), Comte (1975), Smith (1975), and Jensen, Strom, and Strom (1976). In general, the more recent results have confirmed Searle's observation and have supported the interpretation in terms of abundance gradients in N/O and N/S.

Only Searle and Sargent (1972) and Smith (1975) have determined abundance gradients directly, by measuring λ4363 of [O III] and, therefore, the electron temperature which allows the computation of ionic abundances. In all other investigations the line intensity gradients have been modeled in varying degrees of complexity, with the ionizing spectrum, dust content, gas clumpiness, and heavy-element abundances left as free parameters. Shields (1974) modeled the results of Searle and confirmed that abundance gradients were necessary for explaining the [N II]/[O II] and [O III]/Hβ gradients. In these models oxygen is enhanced by more than a factor of 10 from the outermost to the innermost spiral arms. Sarazin (1976) concluded that abundance gradients alone were insufficient to explain the observed line intensity gradients, and his models required a changing gas-to-dust ratio as well. The inner-arm H II regions would have a softer ionizing spectrum if they contained large amounts of dust capable of competing successfully with the gas for ionizing photons. As a result, the magnitude of the enhancement of oxygen in Sarazin's models is somewhat less than that inferred by Shields.

Although the existence of abundance gradients in nitrogen and oxygen in several spiral galaxies is not in doubt, the magnitude of these gradients has been computed directly only for the outer regions of M101 and M33. In general, specific conclusions concerning the amount of enhancement are highly model dependent.

Only recently has the question of abundance gradients from nebulae in our Galaxy been investigated. The bulk of these abundance determinations have been for planetary nebulae (Barker 1978; D'Odorico, Peimbert, and Sabbadin 1976; Aller 1976; Torres-Peimbert and Peimbert 1977). Gradients in nitrogen, oxygen, and helium have been found at varying levels of confidence in one or more of these studies. Two attempts to look for abundance gradients from galactic H II regions have been made. Sivan (1976) has obtained observations of the line ratio [N II]/[S II] in 10 H II regions; Peimbert, Torres-Peimbert, and Rayo (1978) have independently

* *Lick Observatory Bulletin*, No. 797.

† Now at Cerro Tololo Inter-American Observatory, which is operated by the Association of Universities for Research in Astronomy, Inc., under contract with the National Science Foundation.

investigated abundance gradients in five H II regions, incorporating the observations of Peimbert and Costero (1969).

Apart from the work of Peimbert and Costero on M8, M17, and the Orion Nebula, little photoelectric spectrophotometry of galactic H II regions has been published. The primary purpose of this study is to compile line intensities for a larger number of H II regions and to compute physical conditions and chemical abundances. By incorporating published distances to the H II regions, an independent determination can be made as to whether gradients in oxygen, nitrogen, sulfur, neon, or helium exist in the Galaxy. In fact, H II regions offer several advantages over planetaries for examining the question of abundance gradients. Distances to H II regions, derived by the method of spectroscopic parallax, are generally more accurately known than are distances to planetary nebulae. H II regions are extreme Population I objects and, therefore, are composed of material which represents the current composition of the interstellar medium, whereas planetary nebula envelopes represent material which is more than 10^9 years old and is representative of the material in the interstellar medium at the time and place the planetary nebula progenitor formed. Furthermore, the abundances in planetaries can be affected by processing in the progenitor star (Torres-Peimbert and Peimbert 1971). Unfortunately, H II regions are generally of much lower surface brightness than planetary nebulae, making observations, particularly of the faint auroral lines of [O III] and [N II], difficult.

A secondary purpose of this investigation is to obtain more detailed observations of a few extragalactic H II regions in order to deduce the electron temperature from a measurement of [N II] λ5755 where [O III] is weak or absent and to deduce a more accurate sulfur abundance from [S III] λ6312. If magnitudes of abundance gradients can be determined observationally in a galaxy for which there exists a large body of data on line intensity gradients, then some conclusions may be reached as to whether the commonly measured line ratios—[N II]/Hα, [O III]/Hβ, [N II]/[S II], and [N II]/[O II]—really can be used as abundance diagnostics.

Section II outlines the observational methods. Sections III and IV deal with the calculation of physical conditions and ionic and total abundances. Section V considers the question of abundance gradients in the Galaxy and line intensities as abundance indicators, and § VI presents improved abundances for an inner-arm H II region in M101 and a comparison of gradients across M101 to gradients in the Galaxy.

II. OBSERVATIONS

The nebulae in this study were chosen from those in Miller's (1968) program of radial velocity determinations for galactic H II regions. This sample is well suited to a spectrophotometric survey, because it includes a large number of the higher-surface-brightness H II regions whose distances are uniformly and fairly accurately determined. Table 1 lists the nebulae, along with their galactic coordinates and galactocentric distances. Each H II region, except IC 410, has been assigned to a spiral arm—Sagittarius (S), Orion (O), or Perseus (P). The data in Table 1 were taken from Miller (1968).

TABLE 1

TABLE OF NEBULAE OBSERVED

Nebula	l	b	R (kpc)	Spiral Arm
M16	17.0	+0.8	7.9	S
M20	7.0	−0.2	8.5	S
M8	6.1	−1.2	8.6	S
S101	71.6	+2.9	9.5	O
S119	87.2	−3.8	10.0	O
IC 5146 (S125)	94.4	−5.6	10.1	O
NGC 1976	209.1	−19.4	10.4	O
IC 2177 (S292)	223.7	−1.9	10.6	O
S132	102.8	−0.9	11.2	P
NGC 7380 (S142)	107.0	−1.0	11.3	P
NGC 281 (S184)	123.2	−6.3	11.9	P
S261	194.1	−1.9	12.2	P
NGC 2175 (S252)	190.1	+0.6	12.4	P
NGC 2467 (S311)	243.2	+0.3	13.0	O
IC 410 (S236)	173.6	−1.8	13.8	...

The bulk of the observations were obtained with the image-tube scanner (ITS) (Robinson and Wampler 1972; Miller, Robinson, and Wampler 1976) at the Cassegrain focus of the Lick Observatory 3 m Shane reflector. The ITS is a two-channel device, with the slits separated along an east-west line by 35″. Consequently, independent observations of two positions in a nebula could be made simultaneously. A sky scan was taken well away from the nebula and subtracted from the nebula plus sky scan in an attempt to remove the night-sky emission lines. In general, the slits were situated in the highest-surface-brightness parts of the H II regions. A "blue" grating setting ($\lambda\lambda$3700–5800) and a "red" grating setting ($\lambda\lambda$4600–7100) were used to cover the available spectral range. The ultraviolet sensitivity of the ITS is limited by the fiber optics in the "red" image-tube chain, and the infrared sensitivity is limited by the response of the photocathode. Slit sizes of 2.″4 × 4.″0 gave a spectral resolution of about 7 Å FWHM. The raw data were reduced to energy distributions from observations of standard stars calibrated by Stone (1977), which are tied to the calibration of Vega by Hayes and Latham (1975).

Because the observing procedure is to alternate between the nebula plus sky and sky alone, an important consideration is possible errors due to improper repositioning of the slits in the nebula. The television guiding system has a memory which allows the observer to store a picture of the original field; this picture can be subtracted from the current field, and the result can be displayed. Utilizing this technique reduces the repositioning errors to 1″ or less, and this method was employed when a convenient guide star was not available.

Observations of M8 were obtained with an ITS attached to the Cassegrain focus of the Lick Observatory 60 cm telescope. The observing and reduction procedures were similar to those employed at the 3 m

telescope. The slit size at the 60 cm telescope was 8″ × 10″. Four positions were observed in M8. These data were reduced to energy units from observations of the standard star Trumpler 183, which has been calibrated by R. Stone (private communication). Accurate repositioning in the nebula is possible at the 60 cm telescope by using an offset guider.

Observations of the Orion Nebula were obtained with the sequential scanner (Wampler 1966) and the Crossley 90 cm reflector. The entrance slit size was 8″ × 200″. The exit slit for most of the observations, 1 × 5 mm, gave 16 Å resolution in second order and 32 Å in first order. In the wavelength region λλ6300–7000 an exit slit of 0.6 × 5 mm was used in order to resolve Hα + [N II] and [S II] λλ6717, 6731. The detector was a photomultiplier tube with a photocathode of InGaAsP with a usable spectral response from below 3000 Å to near 11000 Å. The observations of the Orion Nebula were made as part of a test of this new photomultiplier tube. The data were flux calibrated by means of observations of a subset of the Hayes (1970) standards. Three positions were observed, and the resulting line intensities are in good agreement with those published by Peimbert and Costero (1969) for similar positions in the Orion Nebula.

I have summarized the information pertaining to the observations in Table 2. For the 3 m observations I have given the offsets for position 1 only. Position 2 is 35″ east of position 1.

The measured line intensities were corrected for reddening by comparing the observed Balmer decrement to that predicted under the assumption of pure recombination (Brocklehurst 1971). The Whitford (1958) reddening law as parametrized by Miller and Mathews (1972) was adopted. The resolution of the ITS is sufficient that Hα was not seriously contaminated by [N II] λλ6548, 6583. This problem will be discussed in more detail in § III. In many, but not all, cases the $E(B-V)$ from the Balmer lines is in good agreement with the $E(B-V)$ published by Miller (1968) for the stars in the nebulae.

Table 3 contains the line intensities on a scale where $I(\mathrm{H}\beta) = 100$. In order to conserve space, only the reddening-corrected fluxes $I(\lambda)$ are given. The estimated errors are 10% or less for the emission lines with $I(\lambda) \geq 100$, 25%–40% for the lines with $10 \leq I(\lambda) < 100$, and about 50% for $I(\lambda) < 10$. These

TABLE 2

JOURNAL OF OBSERVATIONS

NEBULA AND DATE (UT)	TELESCOPE	REFERENCE POINT	OFFSETS (arcsec) Δα	Δδ
M16:				
1976 June 26	3 m	Bright blob to N of Eagle	0	0
M20:				
1976 June 24	3 m	HD 164492	0	−40
M8:				
1977 May 17	60 cm	Hourglass	0	0 (pos. 1)
			0	+100 (pos. 2)
1977 May 18	60 cm	Hourglass	0	−50 (pos. 3)
			0	+50 (pos. 4)
S101:				
1976 June 25	3 m	HD 227018	0	+70
S119:				
1976 October 21–22	3 m	BD +43 3893	+167	−20
IC 5146:				
1976 July 30	3 m	BD +46 3474	−70	−35
NGC 1976:				
1976 November 16–17	90 cm	Bond 628	0	−120 (pos. 1)
			0	+120 (pos. 2)
			−59	+300 (pos. 3)
IC 2177:				
1977 February 19	3 m	HD 53367	0	−154
S132:				
1976 July 30	3 m	BD +55 2722	+90	+90
NGC 7380:				
1976 September 17	3 m	HD 215835	−330	0
NGC 281:				
1976 October 21	3 m	HD 5005	+60	−108
S261:				
1977 January 26	3 m	HD 41997	0	−214
NGC 2175:				
1977 February 18	3 m	HD 42088	+173	−67
NGC 2467:				
1977 April 21	3 m	HD 64315	0	−30
IC 410:				
1976 October 21	3 m	HD 242908	+216	−60

TABLE 3

LINE INTENSITIES IN H II REGIONS

λ	ID	M16 Pos 1 I(λ)	M16 Pos 2 I(λ)	M20 Pos 1 I(λ)	M20 Pos 2 I(λ)	M8 Pos 1 I(λ)	M8 Pos 2 I(λ)	M8 Pos 3 I(λ)	M8 Pos 4 I(λ)	S101 Pos 1 I(λ)	S101 Pos 2 I(λ)	S119 Pos 1 I(λ)	S119 Pos 2 I(λ)	IC5146 Pos 1 I(λ)	IC5146 Pos 2 I(λ)	IC2177 Pos 1 I(λ)	IC2177 Pos 2 I(λ)	Orion Pos 1 I(λ)
3727	[O II]	161	329	308	337	144	185	280	93.0:	187	283	316	223	211	259	243	254	203
3868	[Ne III]	--	6.4:	23.2	3.9	--	4.9:	7.1:	37.3:	33.7	--	--	--	--	--	4.8:	--	26.4
4071	[S II]	3.2:	5.7:	0.9:	0.7:	--	--	--	--	9.3:	--	--	--	--	--	--	--	4.0
4101	Hδ	29.4	29.6	25.2	28.7	15.4	18.4	24.1	23.7	49.1	36.2	29.9	13.7:	20.6	27.1	31.2	32.5	40.7
4340	Hγ	55.9	50.2	54.4	50.7	37.2	39.9	47.1	48.2	65.8	53.6	63.0	63.5	45.1	47.6	50.0	37.4	57.6
4363	[O III]	<4.1	<4.3	--	<4.5	--	0.7:	1.3:	1.8:	--	--	--	--	--	--	--	--	1.2
4861	Hβ	100	100	100	100	100	100	100	100	100	100	100	100	100	100	100	100	100
4922	He I	1.8	1.4	--	1.9	--	--	--	--	4.3	3.2	13.7	10.0	--	--	--	--	--
4959	[O III]	47.0	28.0	25.8	27.5	75.3	45.9	62.1	65.6	16.9	15.9	9.5	4.4	--	--	--	--	101
5007	[O III]	145	92.7	81.2	89.3	200	133	199	190	48.1	48.6	18.5	16.0	--	--	--	--	318
5755	[N II]	0.4	2.4	<1.0	0.8	1.8:	0.8	1.0:	<0.7:	1.3:	--	--	--	--	--	1.3:	--	0.6
5876	He I	11.9	18.1	9.5	10.1	9.9	10.8	12.1	9.3	10.0	9.0	10.1:	14.3:	1.9	4.7	--	--	11.4
6312	[S III]	<0.2	2.2	<0.5	1.2	0.8:	1.3:	1.2:	<0.5:	--	<1.5	--	--	--	--	--	--	1.7
6548	[N II]	16.4	50.2	26.5	24.1	55.9	34.8	33.8	23.6	25.8	21.2	36.0	41.0	34.5	34.0	29.3	30.0	--
6563	Hα	287	287	287	287	287	287	287	287	287	287	287	287	287	287	287	287	287
6583	[N II]	52.2	159	84.0	76.4	114	82.4	91.1	70.5	87.6	73.8	111	125	113	114	91.7	93.3	48.6
6678	He I	2.8	2.4	2.5	2.8	3.0	2.8	3.3	5.0	2.6	1.1:	--	--	--	--	--	--	3.4
6717	[S II]	8.0	22.9	18.5	15.3	13.3	6.7	12.6	5.1	28.4	17.4	47.8	46.3	44.1	33.2	43.7	47.4	2.8
6731	[S II]	7.6	30.0	14.9	13.1	13.0	5.3	13.8	4.7	19.5	14.2	26.5	33.4	32.0	25.8	40.1	30.7	4.9
7065	He I	2.3	1.4	--	--	--	--	--	--	2.6	--	--	--	--	--	--	--	--
7326	[O II]	--	--	--	--	--	--	--	--	--	--	--	--	--	--	--	--	8.6
8446	O I	--	--	--	--	--	--	--	--	--	--	--	--	--	--	--	--	1.0
9532	[S III]	--	--	--	--	--	--	--	--	--	--	--	--	--	--	--	--	74.8
10049	P 7	--	--	--	--	--	--	--	--	--	--	--	--	--	--	--	--	6.0
10830	He I	--	--	--	--	--	--	--	--	--	--	--	--	--	--	--	--	43.1

TABLE 3—*Continued*

λ	ID	Orion Pos 2 I(λ)	Orion Pos 3 I(λ)	S132 Pos 1 I(λ)	S132 Pos 2 I(λ)	NGC7380 Pos 1 I(λ)	NGC7380 Pos 2 I(λ)	NGC281 Pos 1 I(λ)	NGC281 Pos 2 I(λ)	S261 Pos 1 I(λ)	S261 Pos 2 I(λ)	NGC2175 Pos 1 I(λ)	NGC2175 Pos 2 I(λ)	NGC2467 Pos 1 I(λ)	NGC2467 Pos 2 I(λ)	IC410 Pos 1 I(λ)	IC410 Pos 2 I(λ)
3727	[O II]	230	306	118:	366	191	165	248	210	465	429	153	143	197	181	301	192
3868	[Ne III]	24.1	10.1	--	--	8.9	--	30.8:	7.0:	--	--	14.4	--	17.9	--	--	11.7:
4071	[S II]	3.2	3.6	--	--	--	9.1:	--	7.3:	--	--	--	--	--	--	--	--
4101	Hδ	41.1	33.9	45.8	--	37.2	21.2	18.0	33.1	37.9	14.2:	23.9	24.1	23.5	36.0	51.4	42.9:
4340	Hγ	80.0:	50.9	64.5	--	50.9	52.6	51.2	52.0	59.9	42.7	61.2	50.8	60.7	56.2	76.9	33.6
4363	[O III]	1.5	3.1:	--	--	--	--	--	--	--	--	--	--	--	--	--	--
4861	Hβ	100	100	100	100	100	100	100	100	100	100	100	100	100	100	100	100
4922	He I	--	--	--	--	--	--	--	6.0	--	--	--	--	--	--	8.2	--
4959	[O III]	97.1	55.6	21.5	38.6	46.4	44.7	42.1	49.7	13.0	14.3	70.0	65.6	87.9	89.0	66.4	59.2
5007	[O III]	305	175	113	109	121	131	124	148	34.0	29.2	218	206	277	275	199	198
5755	[N II]	0.6	1.0	--	--	--	--	0.4:	--	--	1.6:	--	--	--	--	--	--
5876	He I	17.3:	11.5	20.8:	17.6	9.9	15.0	13.8	16.0	16.5	7.8	16.6	13.5	14.2	12.2	16.7	16.3
6312	[S III]	1.6	1.3	3.2:	--	1.1	1.1:	2.1:	--	4.5	--	--	1.5:	2.6	1.9:	<3.8	--
6548	[N II]	--	--	11.7	8.3:	15.5	13.0	17.8	11.2	33.6	36.5	(4.5)	(8.2)	10.0	11.5	16.6	15.7
6563	Hα	287	287	287	287	287	287	287	287	287	287	287	287	287	287	287	287
6583	[N II]	51.2	91.0	53.1	48.1	46.0	38.7	50.9	42.9	86.4	108	13.4	24.4	29.9	34.2	49.3	42.4
6678	He I	3.5	2.8	--	--	2.6	1.9	8.5	4.2	5.2	--	11.1	--	4.7	2.4	--	--
6717	[S II]	3.1	11.8	17.1	10.1	11.6	9.1	14.2	10.0	28.7	38.4	17.3	14.5	7.6	7.1	12.8	17.4
6731	[S II]	5.2	13.3	7.7	12.7	8.3	8.8	12.8	7.4	23.3	25.0			7.9	5.7	18.3	9.3
7065	He I	--	--	--	--	--	--	--	--	--	--	--	--	4.6	--	--	--
7326	[O II]	11.5	9.5	--	--	--	--	--	--	--	--	--	--	--	--	--	--
8446	O I	1.0	1.7	--	--	--	--	--	--	--	--	--	--	--	--	--	--
9532	[S III]	93.0	99.0	--	--	--	--	--	--	--	--	--	--	--	--	--	--
10049	P 7	7.7	8.2	--	--	--	--	--	--	--	--	--	--	--	--	--	--
10830	He I	41.7	30.2	--	--	--	--	--	--	--	--	--	--	--	--	--	--

estimates result from a comparison of the lines in the overlap region of the two grating settings and from much experience with the instrument. Line intensities followed by a colon may be in error by as much as a factor of 2. Table 4 presents for each position the flux in Hβ, the $E(B-V)$ derived from the Balmer decrement, and the $E(B-V)$ from the stars in the nebula compiled by Miller (1968).

III. DENSITIES, TEMPERATURES, AND IONIC ABUNDANCES

For the purpose of calculating ionic abundances, a knowledge of the temperatures and, in some cases, the densities in the line-emitting regions is needed. Electron densities in gaseous nebulae are typically derived from the ratio $I(\lambda3726)/I(\lambda3729)$ of [O II] or $I(\lambda6717)/I(\lambda6731)$ of [S II]. The resolution of the ITS is insufficient to resolve the [O II] doublet, and so the electron densities were computed from the [S II] lines. Electron temperatures are generally derived from the ratio of auroral to nebular lines in [O III] or [N II].

The dependence of these line ratios on density and temperature was calculated using a multilevel atom program which incorporates transition probabilities and collision strengths given by Osterbrock (1974) except for collision strengths for N^+ and O^{++}, which came from Seaton (1975) and Eissner and Seaton (1974), respectively.

The electron densities derived from the [S II] line ratios were usually near the low-density limit. At this level the derived ionic abundances are insensitive to the exact value of the electron density. In NGC 2175 it was not possible to measure the [S II] lines individually. The uncertainty in the other electron densities is about ± 200 cm^{-3} except for densities followed by a colon, which may be in error by a factor of 2.

Several circumstances conspire to make the observational determination of electron temperatures difficult. First, the galactic H II regions in this study are generally of low surface brightness. Second, because of the proximity of strong night-sky lines at λ4358 and λλ5770, 5791, the auroral lines of [O III] λ4363 and [N II] λ5755 are often contaminated. Third, some H II regions exhibit only very weakly the relevant lines in their spectra. Obviously, only the higher-ionization H II regions will show strong [O III] emission. As a result, in only five H II regions has a reliable observational determination of the electron temperature been made. These are M8, the Orion Nebula, M16, M20, and NGC 281.

In order to obtain an estimate of the electron temperature for the nebulae with [O III] or [N II] temperatures and with a single or dominant ionizing star, I have calculated model H II regions using a program described by Grandi (1975, 1976). This program calculates the thermal and ionization structure of a spherically symmetric H II region surrounding a central ionizing source. The radiation transfer problem is solved in the plane-parallel approximation, and the diffuse radiation is handled by means of the on-the-spot approximation. The spectral types for the ionizing stars were taken from Miller (1968). The corresponding model atmospheres were taken from Mihalas (1972).

Of course, the electron temperatures computed by the models are a function of the assumed abundances. The input abundances were taken to be the average of the abundances for the nebulae with observationally determined temperatures. The effect of the assumed abundances on the model temperatures and on the subsequently derived abundances will be discussed in more detail in § V. Of all the nebulae with observationally determined temperatures, NGC 281 appears to be the least complex. In order to test the validity of using model calculations for estimating electron temperatures, I have computed a model for NGC 281 which has a single ionizing star of spectral type O6. The observed electron temperature is 7750 ± 1000 K. A model of NGC 281 gives a temperature of 8500 K, which implies that the models can accurately estimate the temperature if the input abundances are not far wrong.

With values for the temperatures and densities, the ionic abundances from the forbidden lines can be computed from the following expression:

$$\frac{N(X^+)}{N(H^+)} = \frac{\lambda(\text{Å})}{4861}\left[\frac{S(X)}{P(X,n)}\frac{N_e\alpha(4,2;H^0)}{A}\right]\frac{I(\lambda,X)}{I(H\beta)}. \quad (1)$$

$N(X^+)/N(H^+)$ is the relative number density of ion X; $P(X,n)/S(X)$ is the population of the upper level of the transition relative to the population of all levels in ion X; $\alpha(4,2;H^0)$ is the recombination coefficient for forming Hβ; and A is the transition probability. The ratios $P(X,n)/S(X)$ were computed using the multilevel atom program. Collision strengths and transition probabilities in addition to those mentioned previously came from Osterbrock (1974) except for the collision strength for Ne^{++}, which came from Pradhan (1974).

The He^+ abundances derive from ratios of recombination lines and are therefore less sensitive to errors in the electron temperature determination. The recombination coefficients were taken from Brocklehurst (1971, 1972). No allowance was made for the possible effects of self-absorption or collisional excitation. These effects are not expected to be important in galactic H II regions such as these (Peimbert and Torres-Peimbert 1977). The He^+ abundances were derived from the intensity of λ5876, because it is the only helium line which could be measured with consistently high accuracy. Because of the relative insensitivity of the derived $N(He^+)/N(H^+)$ to the electron temperatures, the errors in the He^+ abundance are essentially the same as the errors in the measured flux in λ5876. In the worst case, this is probably no more than 50%.

The temperature correction procedure of Peimbert and collaborators (Peimbert and Costero 1969; Peimbert and Torres-Peimbert 1971) was not used in the calculation of the ionic abundances. This was due in large part to the fact that generally only one (or no) temperature-sensitive line ratio could be measured

TABLE 4

Hβ FLUX AND REDDENING

Nebula	$F(H\beta)$ ergs cm^{-1} s^{-1}	$E(B-V)_{H\alpha/H\beta}$	$E(B-V)_{stars}$
M16:			
Position 1	3.8×10^{-14}	0.81	...
Position 2	9.8×10^{-14}	0.97	...
M20:			
Position 1	7.6×10^{-14}	0.42	0.25
Position 2	7.1×10^{-14}	0.48	0.18
			0.31
M8:			
Position 1	2.0×10^{-12}	0.42	0.35
Position 2	1.2×10^{-11}	0.38	0.30
Position 3	4.0×10^{-13}	0.37	0.41
Position 4	3.3×10^{-13}	0.27	...
S101:			
Position 1	5.6×10^{-15}	0.73	0.70
Position 2	7.0×10^{-15}	0.84	...
S119:			
Position 1	2.4×10^{-15}	0.27	0.31
Position 2	4.6×10^{-15}	0.12	...
IC 5146:			
Position 1	9.3×10^{-15}	0.49	1.04
Position 2	9.4×10^{-15}	0.59	...
Orion:			
Position 1	4.2×10^{-10}	0.43	0.36*
Position 2	3.6×10^{-10}	0.37	...
Position 3	6.4×10^{-11}	0.15	...
IC 2177:			
Position 1	1.1×10^{-14}	0.24	0.74
Position 2	9.0×10^{-15}	0.44	...
S132:			
Position 1	3.6×10^{-15}	0.89	0.43
Position 2	3.8×10^{-15}	0.96	0.57
			0.49
NGC 7380:			
Position 1	5.4×10^{-15}	0.77	0.59
Position 2	6.7×10^{-15}	0.68	0.66
			0.65
			0.79
NGC 281:			
Position 1	6.7×10^{-15}	0.48	0.40
Position 2	1.0×10^{-14}	0.59	...
S261:			
Position 1	3.5×10^{-15}	0.91	0.70
Position 2	6.6×10^{-15}	0.94	...
NGC 2175:			
Position 1	1.8×10^{-14}	0.31	0.39
Position 2	1.7×10^{-14}	0.40	0.83
NGC 2467:			
Position 1	3.1×10^{-14}	0.61	0.57
Position 2	3.0×10^{-14}	0.67	0.51
			0.57
			0.61
			0.43
IC 410:			
Position 1	6.1×10^{-15}	0.53	0.60
Position 2	7.3×10^{-15}	0.66	0.66
			0.51

* $E(B-V)$ for θ^1 Ori (ABCD) from Lee 1968; all other $E(B-V)$ from Miller 1968.

in a given nebula. In the presence of temperature fluctuations, the temperature determined from the forbidden lines will be an overestimate of the temperature that is characteristic of the region giving rise to the emission (Peimbert 1967). Consequently, the derived ionic abundances will tend to be lower limits to the true abundances. A comparison of abundances derived with and without temperature fluctuations indicates that this difference amounts to 0.2–0.3 dex. These remarks are applicable to abundances all of ionic species except He^+.

In attempting to model the ionization structure of an H II region, one typically makes the assumption of two distinct ionization zones. One zone contains the low-ionization species—O^+, N^+, S^+, and S^{++}. The other contains the high-ionization species—O^{++} and

Ne^{++}. In this model, T_e([O III]) would be appropriate for the calculation of ionic abundances in the one zone and T_e([N II]) in the other. Unfortunately, because of the difficulties mentioned previously, only in M8 and the Orion Nebula are both temperatures available. The temperature from [N II] is often the only one observable because of the low ionization of H II regions and the larger ratio of auroral to nebular lines at a given temperature. Consequently, systematic errors in the abundances of O^{++} and Ne^{++} will be introduced unless the temperatures in the high- and low-ionization zones are the same. The model calculations indicate that the two temperatures differ by something like 1000 K, with the [O III] temperature being lower. This agrees with the model calculations published by Balick and Sneden (1976), although the observations of the Orion Nebula—and with less accuracy, of M8—indicate that the difference may not be so great. If the temperature in the high-ionization zone is really lower than the value used, the O^{++} and Ne^{++} abundances will be underestimates of the true abundances.

Other sources of error will be discussed in the context of each ion. The derived abundance of O^+ is more strongly influenced by the adopted electron density than are those of the other ions, although this dependence is not great. A factor of 2 change in the electron density will change the O^+ abundance by less than 20%. The abundance is based on the intensity of λ3727, which is usually strong in H II regions. The errors associated with the measurement of λ3727 are slightly greater than those associated with other lines of comparable intensity, because the "red" image-tube chain used for these observations lacks ultraviolet sensitivity; therefore the flux calibration below λ4000 is somewhat less certain. Also, the correction for atmospheric extinction is large at these wavelengths. Still, the largest uncertainty in the O^+ abundances is introduced by the uncertain electron temperature. An error of 1000 K in T_e changes the O^+ abundance by roughly a factor of 2.

There are primarily two sources of error in the O^{++} abundance in addition to the possible systematic error discussed previously. In the low-ionization H II regions the measurement of [O III] is uncertain by approximately 25%. The largest error in the O^{++} abundance is caused by the temperature error. A change of 1000 K in T_e causes a change of about 50% in the derived abundance of O^{++}.

An additional source of error associated with the N^+ abundance determination is the measurement of λλ6548, 6583 of [N II]. Because of the proximity of these lines to Hα, blending may result when all three lines are strong. By using a computer program devised for the purpose by A. T. Koski, the blend can be synthesized from an unblended profile (say, Hβ) which has been translated in wavelength and scaled in intensity. This more involved procedure did not give answers significantly different from the less complex approach of a simple eye estimate of the relative intensities. A check on the line intensity measurements may be made by comparing the observed ratio $I(\lambda6583)/I(\lambda6548)$ to the value 2.98 which is fixed by the atomic constants. For NGC 2715, $I(\lambda6548)$ was not measured and was taken to be $I(\lambda6583)/3$. The principal source of error in the N^+ abundance again results from an imprecise knowledge of the electron temperature. A change of 1000 K in T_e implies a change in the abundance of N^+ of about 50%.

Errors in the line intensities are more important in the determination of the Ne^{++} abundance, which is based solely on λ3868. Because of the high ionization potential of Ne^+ (41 eV), very little neon is in the form of Ne^{++}; consequently, the line is weak. Furthermore, λ3868 falls in a region of the spectrum where the data tend to be noisier as mentioned previously. The error in the measurement of λ3868 can be as much as a factor of 2–5. However, an effort was made to measure this line in every nebula, because the neon abundance has previously been determined from the optical lines in only one H II region, the Orion Nebula. The error introduced by the temperature is much the same as for O^{++}. A change of 1000 K in T_e results in a change in $N(Ne^{++})/N(H^+)$ of roughly a factor of 2.

The determination of the S^+ abundance is based on $I(\lambda6717 + \lambda6731)$; these lines are usually strong enough to be reliably measured. The S^+ abundance is slightly dependent on the electron density, but it is less sensitive than the O^+ abundance. Errors introduced by the electron density will be ignored. The effect of errors in the electron temperature is to change the derived S^+ abundance by approximately 50% for a 1000 K change in T_e.

Critical to the determination of the total sulfur abundance is the S^{++} ionic abundance. This will be discussed in more detail below. The strong nebular lines of [S III] λλ9069, 9532 are inaccessible owing to the lack of infrared sensitivity of the ITS. In only one H II region (the Orion Nebula) were they measured with the infrared-sensitive photomultiplier tube and the Crossley scanner. The auroral line of [S III] is at λ6312. This spectral region is contaminated by [O I] in the nebula and in the sky and by OH from the night sky. Consequently, the measurement of λ6312 is difficult, and the errors in the line intensities range from 50% to 100%. Even with the larger uncertainty in the line fluxes, the principal source of error results from the electron temperature determination. The calculated S^{++} abundance will change by roughly a factor of 2 for a 1000 K change in T_e. All of the densities, temperatures, and ionic abundances are given in Table 5. The electron temperatures followed by (O) are observed temperatures; those followed by (M) are model temperatures. Unless otherwise indicated, the temperatures are from [N II]. Two nebulae are not included in Table 5. NGC 7380 does not have an observed electron temperature and was more complicated to model than were the other H II regions. S132 was not included, because it is one of the nebulae with the lowest surface brightness, and the line intensities were therefore less accurately known; this was particularly true for λ3727, which is necessary for a determination of the O^+ abundance, which is in turn necessary for the calculation of the total abundance

TABLE 5

TEMPERATURES, DENSITIES, AND ABUNDANCES

	M16		M20		M8		S101		S119		IC5146
	Pos 1	Pos 2	Pos 1	Pos 2	Pos 2	Pos 3	Pos 1	Pos 2	Pos 1	Pos 2	Pos 1
T_e (°K)	7,700°(0)	7,900°(0)	9,000°(0)	8,600°(0)	8,150°(0) 9,350°(0)†	8,600°(0)	8,250°(M)	8,250°(M)	7.570°(M)	7,570°(M)	5,500 °(M)
N_e (cm^{-3})	1,000	3,000	400	600	400	1600	100	400	100	100	100
He^+	.079	.063	.068	.068	.076	.086	.070	.063	.080:	.113:	.012
i_{cf}	1.27	2.45	1.97	1.61	1.32	1.39		2.14			
He	.100	.154	.134	.110	.100	.119		.135			
O^+	2.4×10^{-4}	5.6×10^{-4}	1.9×10^{-4}	1.7×10^{-4}	2.1×10^{-4}	2.5×10^{-4}	1.7×10^{-4}	2.5×10^{-4}	4.7×10^{-4}	3.3×10^{-4}	9.5×10^{-4}
O^{++}	1.3×10^{-4}	6.3×10^{-5}	3.8×10^{-5}	4.9×10^{-5}	9.3×10^{-5}	1.1×10^{-4}	3.1×10^{-5}	3.1×10^{-5}	2.0×10^{-5}	1.4×10^{-5}	
O	3.7×10^{-4}	6.2×10^{-4}	2.3×10^{-4}	2.2×10^{-4}	3.0×10^{-4}	3.6×10^{-4}	2.0×10^{-4}	2.8×10^{-4}	4.9×10^{-4}	3.4×10^{-4}	9.5×10^{-4}
N^+	2.2×10^{-5}	6.1×10^{-5}	2.2×10^{-5}	2.5×10^{-5}	3.0×10^{-5}	2.8×10^{-5}	2.9×10^{-5}	2.5×10^{-5}	5.0×10^{-5}	5.6×10^{-5}	1.0×10^{-4}
i_{cf}	1.52	1.11	1.20	1.30	1.46	1.44	1.17	1.12	1.04	1.03	1.00
N	3.3×10^{-5}	6.7×10^{-5}	2.6×10^{-5}	3.3×10^{-5}	9.5×10^{-5}	4.1×10^{-5}	3.4×10^{-5}	2.8×10^{-5}	5.2×10^{-5}	5.8×10^{-5}	1.0×10^{-4}
Ne^{++}		1.7×10^{-5}	3.4×10^{-5}	7.0×10^{-6}	1.1×10^{-5}	1.3×10^{-5}	7.4×10^{-5}				
i_{cf}	2.94	9.90	6.09	4.42	3.19	3.29	3.87	9.03	24.5	24.3	
Ne		1.7×10^{-4}	2.1×10^{-4}	3.1×10^{-5}	3.6×10^{-5}	4.2×10^{-5}	2.9×10^{-4}				
S^+	1.0×10^{-6}	3.5×10^{-6}	1.3×10^{-6}	1.3×10^{-6}	6.4×10^{-7}	1.3×10^{-6}	2.4×10^{-6}	1.6×10^{-6}	4.7×10^{-6}	5.0×10^{-6}	1.1×10^{-5}
S^{++}	2.2×10^{-6}:	9.0×10^{-6}	2.8×10^{-6}:	4.9×10^{-6}	1.1×10^{-5}	8.4×10^{-6}		1.3×10^{-5}:			
i_{cf}	1.52	1.11	1.20	1.30	1.46	1.44	1.17	1.12	1.04	1.03	1.00
S	4.9×10^{-6}:	1.4×10^{-5}	4.9×10^{-6}:	8.1×10^{-6}	1.8×10^{-5}	1.4×10^{-5}		1.6×10^{-5}:			1.1×10^{-5}:

† T_e from [O III]

TABLE 5—*Continued*

	IC5146	ORION NEBULA			IC2177		NGC281		S261		NGC2175
	Pos 2	Pos 1	Pos 2	Pos 3	Pos 1	Pos 2	Pos 1	Pos 2	Pos 1	Pos 2	Pos 1
T_e (°K)	5,500°(M)	9,100°(0)	8,900°(0)	8,700°(0)	7,000°(M)	7,000°(M)	7,750°(0)	8,000°*	8,250°(M)	8,250°(M)	9,000°(M)
		8,500°(0)†	9,200°(0)†								
N_e (cm^{-3})	300	8,000	6,000	1,700	800	100	700	200	400	100	
He^+	.026	.082	.125:	.082			.078	.111	.116:	.055	.120
i_{cf}		1.28	1.30	1.49			1.52		2.50	(2.50)*	
He		.105	.163:	.122			.119		.288:	.138	
O^+	1.2×10^{-3}	2.8×10^{-4}	3.0×10^{-4}	2.8×10^{-4}	5.1×10^{-4}	5.3×10^{-4}	3.5×10^{-4}	2.9×10^{-4}	4.2×10^{-4}	3.9×10^{-4}	1.0×10^{-4}
O^{++}		1.5×10^{-4}	1.5×10^{-4}	9.2×10^{-5}			9.6×10^{-5}	1.1×10^{-4}	2.3×10^{-5}	2.1×10^{-5}	1.0×10^{-4}
O	1.2×10^{-4}	4.3×10^{-4}	4.5×10^{-4}	3.7×10^{-4}	5.1×10^{-4}	5.3×10^{-4}	4.4×10^{-4}	4.0×10^{-4}	4.4×10^{-4}	4.1×10^{-4}	2.0×10^{-4}
N^+	1.0×10^{-4}	1.2×10^{-5}	1.4×10^{-5}	2.7×10^{-5}	5.2×10^{-5}	5.3×10^{-5}	2.1×10^{-5}	1.7×10^{-5}	3.1×10^{-5}	3.8×10^{-5}	3.5×10^{-6}
i_{cf}	1.00	1.53	1.48	1.34	1.00	1.00	1.28	1.39	1.05	1.05	2.00
N	1.0×10^{-4}	1.9×10^{-5}	2.0×10^{-5}	3.5×10^{-5}	5.2×10^{-5}	5.3×10^{-5}	2.7×10^{-5}	2.3×10^{-5}	3.2×10^{-5}	4.0×10^{-5}	7.0×10^{-6}
Ne^{++}		4.0×10^{-5}	3.3×10^{-5}	1.7×10^{-5}			9.2×10^{-5}	1.8×10^{-5}			
i_{cf}		2.89	3.06	3.97			4.62	3.58	19.1	19.5	2.00
Ne		1.1×10^{-4}	1.0×10^{-4}	6.8×10^{-5}			4.3×10^{-4}	6.6×10^{-5}			
S^+	8.9×10^{-6}	5.0×10^{-7}	5.0×10^{-7}	1.4×10^{-6}	6.9×10^{-6}	6.4×10^{-6}	1.7×10^{-6}	1.1×10^{-6}	2.7×10^{-6}	3.2×10^{-6}	7.1×10^{-7}
S^{++}		9.5×10^{-6}	9.0×10^{-6}	8.6×10^{-6}			2.2×10^{-5}:		3.8×10^{-5}		
i_{cf}	1.00	1.53	1.48	1.34	1.00	1.00	1.28	1.39	1.05	1.05	2.00
S	8.9×10^{-6}:	1.5×10^{-5}	1.4×10^{-5}	1.3×10^{-5}			3.0×10^{-5}:		4.2×10^{-5}		

† T_e from [O III]

* adopted by analogy with Pos 1.

TABLE 5—*Continued*

	NGC2175	NGC2467		IC410	
	Pos 2	Pos 1	Pos 2	Pos 1	Pos 2
T_e (°K)	9,000°(M)	9,000°(M)	9,000°(M)	9,750°(M)	9,600°(M)
N_e (cm^{-3})		1,500	400	4,000:	100
He^+	.097	.102	.088	.123	.119
i_{cf}		1.15	1.14		
He		.117	.101		
O^+	9.3×10^{-5}	1.3×10^{-4}	1.2×10^{-4}	1.4×10^{-4}	7.7×10^{-5}
O^{++}	9.5×10^{-5}	1.3×10^{-4}	1.3×10^{-4}	7.3×10^{-5}	6.8×10^{-5}
O	1.9×10^{-4}	2.6×10^{-4}	2.5×10^{-4}	2.1×10^{-4}	1.5×10^{-5}
N^+	6.4×10^{-6}	7.8×10^{-6}	8.9×10^{-6}	1.0×10^{-5}	9.3×10^{-6}
i_{cf}	2.02	2.00	2.06	1.52	1.89
N	1.3×10^{-5}	1.6×10^{-5}	1.8×10^{-5}	1.5×10^{-5}	1.8×10^{-5}
Ne^{++}		2.7×10^{-5}			1.3×10^{-5}
i_{cf}	1.98	2.00	1.95	2.88	2.21
Ne		5.4×10^{-5}			2.8×10^{-5}
S^+	6.0×10^{-7}	6.4×10^{-7}	5.3×10^{-7}	1.0×10^{-6}	8.3×10^{-7}
S^{++}		1.4×10^{-5}	1.1×10^{-5}		
i_{cf}	2.02	2.00	2.06	1.52	1.89
S		3.0×10^{-5}	2.3×10^{-5}		

of oxygen, nitrogen, neon, and sulfur as will be described in § IV.

IV. TOTAL ABUNDANCES

In order for one to deduce the total abundance of an element from the abundance of one ionic species, some assumptions must be made concerning the ionization structure of H II regions. As an alternative to detailed model calculations, the ionization correction formulae introduced by Peimbert and collaborators (Peimbert and Costero 1969; Peimbert and Torres-Peimbert 1971) are usually adopted. These formulae make use of the coincidences in the ionization potentials (IP) of several ionic species. The physical assumption is that the ionization distribution of oxygen is a good guide to the ionization distribution of other elements. For example, since $IP(O^+) \approx IP(N^+)$, by implication $N(O^+)/N(O) \approx N(N^+)/N(N)$. The full set of formulae are

$$\frac{N(O)}{N(H)} = \frac{N(O^+ + O^{++})}{N(H^+)}, \tag{2}$$

$$\frac{N(N)}{N(H)} = \frac{N(N^+)}{N(H^+)}\frac{N(O)}{N(O^+)}, \tag{3}$$

$$\frac{N(Ne)}{N(H)} = \frac{N(Ne^{++})}{N(H^+)}\frac{N(O)}{N(O^{++})}, \tag{4}$$

and

$$\frac{N(S)}{N(H)} = \frac{N(S^+ + S^{++})}{N(H^+)}\frac{N(O)}{N(O^+)}. \tag{5}$$

The accuracy of formulae (2)–(5) as they apply to H II regions has been discussed by several authors (Balick

and Sneden 1976; Peimbert and Torres-Peimbert 1977; Hawley and Miller 1977, 1978; Grandi and Hawley 1978). In particular, the model results of Grandi and Hawley indicate that, except for equation (4), the ionization correction scheme does not introduce errors larger than a factor of 2. This is the size of the scatter seen by Hawley and Miller (1977, 1978) in the derived abundances of oxygen, nitrogen, and sulfur in the Ring and Dumbbell Nebulae. The evidence indicates that, in the worst case, formulae (2)–(5) introduce errors in the total abundances about the same size as those due to weak line intensities and the uncertain T_e.

Since the ionization potential of He^0 is 24.6 eV, we must allow for the presence of neutral helium in the H II region. This is illustrated in Figure 1, where the He^+ abundance is plotted against log [O II]/[O III]. Clearly the He^+ abundance correlates with ionization. I infer from this plot that neutral helium is present to some extent in all but the most highly ionized H II regions.

Peimbert and Costero (1969) devised a correction formula based on their observations of the Orion Nebula:

$$\frac{N(\mathrm{He})}{N(\mathrm{H})} = \frac{N(\mathrm{He}^+)}{N(\mathrm{H}^+)} \times \left[0.13\,\frac{N(\mathrm{O})}{N(\mathrm{O}^{++})} + 0.87\,\frac{N(\mathrm{S})}{N(\mathrm{S}) - N(\mathrm{S}^+)}\right]. \quad (6)$$

Obviously this formula is applicable to only those H II regions for which the sulfur abundance is determined. A slight modification to this formula was used by Peimbert and Torres-Peimbert (1977). Peimbert, Rodriguez, and Torres-Peimbert (1974) have argued from model calculations that the ionization correction formula for helium is density dependent, and so equation (6) may not necessarily hold for objects with density distributions different from that of the Orion Nebula. Nevertheless, I have used equation (6) to correct for neutral helium in every nebula with a sulfur abundance determination.

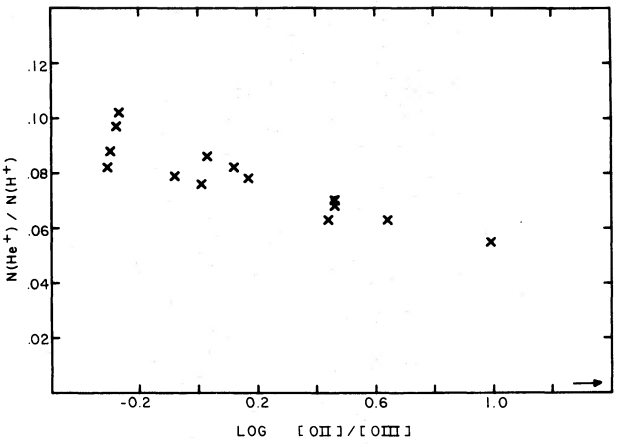

FIG. 1.—Correlation between He^+ abundance and ionization as indicated by the ratio log [O II]/[O III].

It is difficult to assess the accuracy of equation (6). It has not been tested in the manner of equations (2)–(5), because it was fitted to the set of observations of the Orion Nebula in order to minimize the scatter in the total helium abundances. I estimate the total uncertainty in the final helium abundances to be about 10%–20%.

The ionization correction factors and the total abundances are included in Table 5. I have reobserved M8 and the Orion Nebula in order to check my methods and in order to have the whole set of reductions on a consistent set of atomic data. The total abundances for M8 and the Orion Nebula generally agree with those given by Peimbert, Torres-Peimbert, and Rayo (1978). I have compared the abundances to their results for $t^2 = 0.00$, which reduces the temperature fluctuation method to the two-zone approximation.

TABLE 6

TOTAL ABUNDANCES

Nebula	O	N	Ne	S	He
M16	8.70	7.70	8.23*	7.15*	11.10
M20	8.35	7.47	8.08	6.91*	11.09
M8	8.52	7.83	7.59	7.20	11.04
S101	8.38	7.49	8.46†	7.20:†	11.13†
S119	8.62	7.74	...	...	...
IC 5146	9.03	8.00	...	7.00:	...
Orion	8.62	7.39	7.97	7.15	11.05‡
IC 2177	8.72	7.72	...	...	...
NGC 281	8.63	7.40	8.39	7.48:†	11.06
S261	8.63	7.56	...	7.62†	11.14†
NGC 2175	8.29	7.00	...	...	(11.04)
NGC 2467	8.41	7.23	7.73†	7.42	11.04
IC 410	8.26	7.22	7.45*	...	(11.08)
Average	8.60	7.59	8.10	7.26	11.07

* Position 2 only.

† Position 1 only.

‡ Positions 1 and 3 only.

In Table 6 I have summarized the abundances on a logarithmic scale where log $H = 12.00$. All the positions listed in Table 5 for each nebula have been averaged unless otherwise indicated. The helium abundances shown in parentheses in Table 6 are He^+ abundances for nebulae in which the ionization is sufficiently high that almost all helium is once-ionized. At the bottom of each column is the average abundance of each element. The average neon abundance in my sample of H II regions is greater by 0.2 dex than the neon abundance in the Orion Nebula, but the uncertainties are large. The other average abundances are in excellent agreement with recent results for the Orion Nebula (Peimbert and Torres-Peimbert 1977). In particular, the average helium abundance agrees well with that considered typical of galactic planetary nebulae; two recent determinations give 11.06 (Barker 1978) and 11.04 (Torres-Peimbert and Peimbert 1977). The total helium abundance is insensitive to the reduction procedure, i.e., to the choice of t^2. The data presented here are consistent with the statement that there is no difference in the helium abundance between galactic planetary nebulae and H II regions.

V. ABUNDANCE GRADIENTS

The data in Tables 1 and 6 may be used to investigate the possible dependence of abundance on galactocentric distance. The errors in the abundances of neon and sulfur are large enough to preclude a statement concerning possible gradients, so only helium, oxygen, and nitrogen will be discussed.

The results for helium are shown in Figure 2. The squares represent nebulae with observationally determined electron temperatures; the crosses are nebulae with model temperatures. There is no evidence in these data for a dependence of the helium abundances on galactocentric distance.

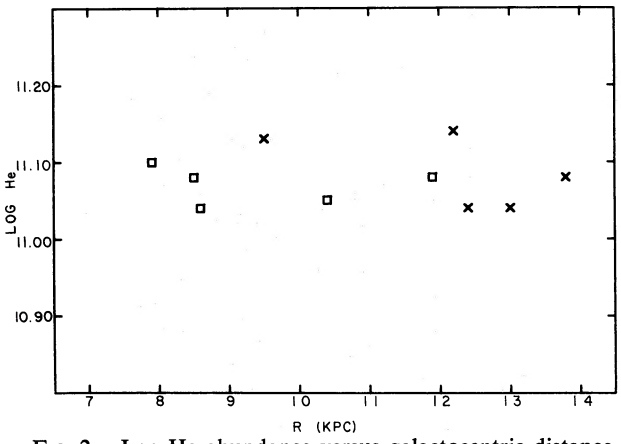

FIG. 2.—Log He abundance versus galactocentric distance (R). Squares represent H II regions with observed electron temperatures; crosses represent H II regions with model electron temperatures.

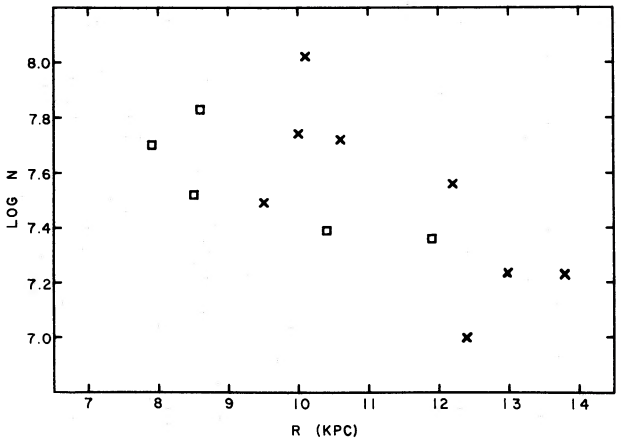

FIG. 3.—Nitrogen abundance versus galactocentric distance for 13 galactic H II regions. The data are taken from Tables 1 and 6.

The nitrogen data are presented in Figure 3. The nitrogen abundance appears to increase with decreasing galactocentric distance. The symbols have the same meaning as in Figure 2. A least-squares solution weighting the points equally gives a magnitude for the gradient $d(\log \mathrm{N/H})/dr = -0.10 \pm 0.03\ \mathrm{kpc}^{-1}$.

The oxygen data are presented in Figure 4. Any gradient in the oxygen abundance is certainly less steep than the nitrogen gradient. A least-squares fit to all the points with equal weighting gives $d(\log \mathrm{O/H})/dr = -0.04 \pm 0.03\ \mathrm{kpc}^{-1}$. Excluding M20 ($R = 8.5$ kpc), which at first glance appears to be the most discordant, and refitting to the data yields $d(\log \mathrm{O/H})/dr = -0.06 \pm 0.03\ \mathrm{kpc}^{-1}$. Possibly the temperature determination for M20 is in error. If the temperature were really 1000 K lower (nearer 8000 K), then the oxygen abundance in M20 would be very nearly equal to the oxygen abundance in M8 ($R = 8.6$ kpc). The electron temperature is certainly less accurately determined in M20 than in M8, M16, or the Orion Nebula.

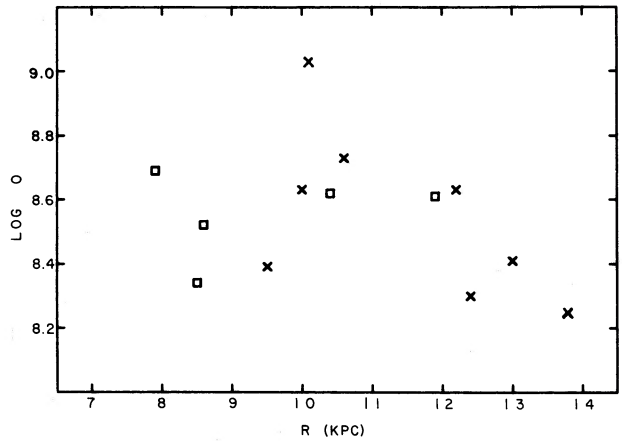

FIG. 4.—Oxygen abundance as a function of galactocentric distance for 13 galactic H II regions. The data are taken from Tables 1 and 6.

The errors in the abundances have been discussed in §§ III and IV. Errors in the distance determinations could tend to confuse whatever abundance gradients might be present. However, according to Miller (1968), the heliocentric distances are probably accurate to ~25% and, therefore, the determinations of the magnitudes of the gradients should not be seriously affected. A potential source of systematic error is the model calculations. Because of the way the input abundances were chosen, the oxygen abundances for the inner H II regions will be underestimated and for the outer H II regions will be overestimated in the presence of a strong oxygen gradient. Consequently, the model electron temperatures will be overestimates for the inner H II regions and underestimates for the outer H II regions. As a result, the abundances in Table 6 would be too small in the direction of the galactic center and too large toward the anticenter. Therefore, the abundance gradients I have presented in this section may be lower limits to the true gradients. Based on a comparison of my results with the results of Peimbert, Torres-Peimbert, and Rayo (1978) for NGC 2467, this effect is not likely to be large.

Ratios of abundances from forbidden lines are less sensitive to the electron temperature determination. It is useful, therefore, to investigate the ratio N/O versus galactocentric distance. This is shown in Figure 5, where log N/O is plotted against R. Errors in log N/O are on the order of ± 0.05 to ± 0.10 dex. The ratio N/O clearly increases with decreasing R. A least-squares fit to the data in Figure 5 gives $d(\log \mathrm{N/O})/dr = -0.06 \pm 0.02\ \mathrm{kpc}^{-1}$.

In Figure 6, I plot log N versus log O. A fit to these data yields the relative enhancement of nitrogen with respect to oxygen. I obtain $\Delta \log \mathrm{N}/\Delta \log \mathrm{O} = 1.1 \pm 0.3$. This agrees well with the result of Peimbert, Torres-Peimbert, and Rayo (1978), $\Delta \log \mathrm{N}/\Delta \log \mathrm{O} = 1.13$. Their value excludes S298. Smith (1975) finds a value of ~1.5 from his extragalactic H II regions. Planetary nebulae (Torres-Peimbert and Peimbert 1977) give $\Delta \log \mathrm{N}/\Delta \log \mathrm{O} = 2.5$. All of these results support the general belief that nitrogen is at least partially a secondary element, probably returned to the interstellar medium through planetary nebula envelopes (Torres-Peimbert and Peimbert 1971).

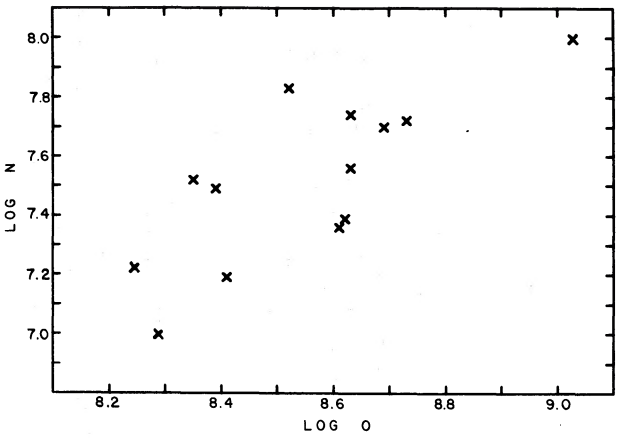

FIG. 6.—Relative enhancement of nitrogen with respect to oxygen.

Figure 7 shows the ratio $\mathrm{N}^+/\mathrm{S}^+$ versus galactocentric distance. Sivan (1976) found a gradient in [N II]/[S II] on the basis of observations of 10 galactic H II regions and argued that this was evidence for an N/S abundance gradient. The extent to which the ratio $\mathrm{N}^+/\mathrm{S}^+$ can be used as a measure of N/S will be discussed below. A least-squares fit to the data in Figure 7 gives $d(\log \mathrm{N}^+/\mathrm{S}^+)/dr = -0.05 \pm 0.02\ \mathrm{kpc}^{-1}$.

Hawley and Grandi (1977) and Peimbert, Rodriguez, and Torres-Peimbert (1974) have shown that N^+ coexists with S^+ and S^{++} in H II regions. Consequently, the assumption used by Sivan (1976) and others that $\mathrm{N}^+/\mathrm{S}^+ \approx \mathrm{N/S}$, based on observations of the inner H II regions in M33 by Benvenuti, D'Odorico, and Peimbert (1973), does not apply. Hawley and Grandi showed that several processes may affect

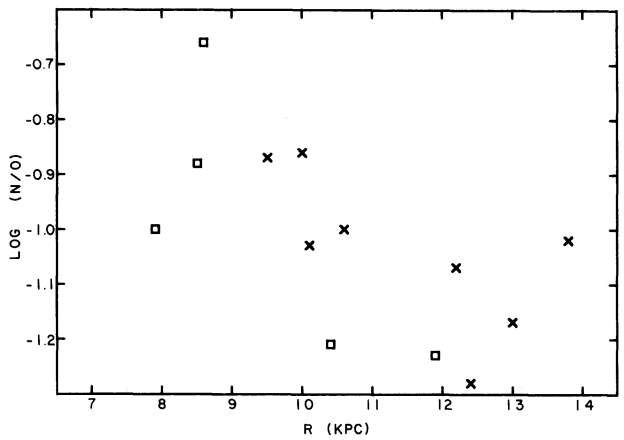

FIG. 5.—Nitrogen to oxygen abundance ratio as a function of galactocentric distance for 13 galactic H II regions. Data are from Tables 1 and 6.

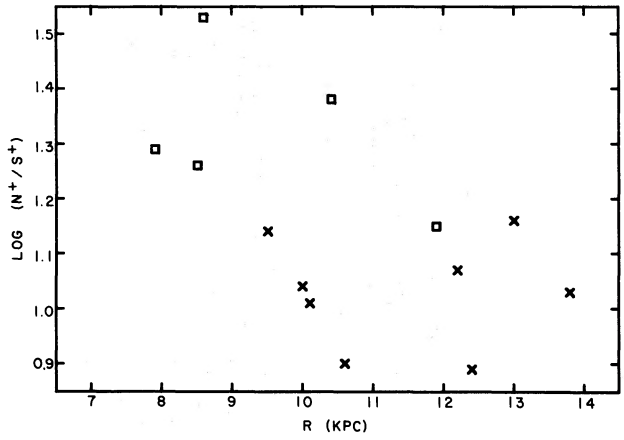

FIG. 7.—N^+ to S^+ abundance ratio as a function of galactocentric distance in 13 galactic H II regions. The data come from Tables 1 and 5.

[N II]/[S II] gradients in addition to abundance gradients and that these other effects seem to work in the opposite sense; i.e., an observed [N II]/[S II] gradient could be taken as a lower limit to the true N/S gradient. Based on the results of that paper, [N II]/[S II] reflects well an N/S abundance gradient, if S^+/S^{++} is a constant for a wide range of ionization and if there are no large systematic trends in oxygen abundance with galactocentric distance. If S^+/S^{++} is a constant, then the agreement between $d(\log N/O)/dr$ and $d(\log N^+/S^+)/dr$ implies that the oxygen and sulfur gradients in the Galaxy are similar. A weak oxygen gradient has only a small effect on the proportionality between [N II]/[S II] and N/S (Hawley and Grandi 1977).

Peimbert, Torres-Peimbert, and Rayo (1978) also find agreement between $d(\log N/O)/dr$ and $d(\log N^+/S^+)/dr$. Their argument that the N^+/S^+ gradient is a good measure of an N/S gradient, based on the similarity of the S/O ratio in Orion, Carina, LMC, and SMC H II regions, implies $N/O \propto N/S$. The data presented in Peimbert and Torres-Peimbert (1976) do not support with confidence the statement that S/O in the LMC and SMC is the same as in the Orion Nebula, and the errors associated with the sulfur abundances in Table 6 are sufficiently large that the S/O ratio in the H II regions in this sample cannot be said to be constant to better than a factor of 2. More accurate observations of [S III] will provide the best way of determining the relative sizes of the oxygen and sulfur gradients.

Although the results of this paper show no evidence of a helium abundance gradient, two studies have proposed such a gradient. Torres-Peimbert and Peimbert (1977) found a helium abundance gradient from planetary nebulae, and Peimbert, Torres-Peimbert, and Rayo (1978) found a similar result from four of their five H II regions. (They did not include their results for M8.) The magnitude of the gradient in both samples implies an increase of roughly 30% in the helium abundance over the baseline which I have observed. Certainly, a change much smaller than 30% or so would be masked by the uncertainties. Churchwell *et al.* (1977) have inferred a helium gradient in agreement with the value quoted above from radio recombination line observations of H II regions. Because of the difficulty in allowing for the presence of neutral helium in H II regions, the question of whether there is a small decrease in the helium abundance with increasing distance from the galactic center probably must remain an open one. The results based on observations of planetary nebulae in which both He^+ and He^{++} are measured are more reliable than results for H II regions, but the interpretation in terms of galactic structure is less clear.

Oxygen abundance gradients have been found from planetary nebulae by Torres-Peimbert and Peimbert (1977) and from five H II regions by Peimbert, Torres-Peimbert, and Rayo (1978). The planetaries yield $d(\log O/H)/dr = -0.06 \pm 0.02\ \mathrm{kpc}^{-1}$, while the H II regions give $d(\log O/H)/dr = -0.13 \pm 0.04\ \mathrm{kpc}^{-1}$. There is no significant difference between the magnitude of the oxygen gradient for planetaries and my results for H II regions. The extent to which the results of Peimbert, Torres-Peimbert, and Rayo (1978) conflict with the results in this paper is not clear. This study includes more than twice as many nebulae as did Peimbert, Torres-Peimbert, and Rayo, including three of their five. Two of these give results in agreement with theirs; the third, NGC 2467 (S311), differs by 0.4 dex in the oxygen abundance. This discrepancy is due primarily to the difference in the electron temperature. My model calculations give $T = 9000$ K, whereas Peimbert, Torres-Peimbert, and Rayo observe $T_e([O\ III]) = 11{,}150$ K. Because of the low altitude at which this object must be observed from Mount Hamilton, contamination of λ4363 by λ4358 is serious and I am unable to confirm their T_e result. Adopting $T_e = 11{,}150$ K and recomputing the abundances in NGC 2467, I obtain $\log O = 8.03$ and $\log N = 7.06$. Incorporating these new values into the least-squares fits gives gradients $d(\log O/H)/dr = -0.06 \pm 0.04\ \mathrm{kpc}^{-1}$ using all points, and $d(\log O/H)/dr = -0.08 \pm 0.04\ \mathrm{kpc}^{-1}$ without M20. The different nitrogen abundance does not significantly change the value of the nitrogen abundance gradient.

Torres-Peimbert and Peimbert (1977) and Peimbert, Torres-Peimbert, and Rayo (1978) have found nitrogen abundance gradients from planetary nebulae and H II regions, respectively. The result for planetaries is $d(\log N/H)/dr = -0.18 \pm 0.04\ \mathrm{kpc}^{-1}$, while four H II regions (excluding S298) give $d(\log N/H)/dr = -0.23 \pm 0.06\ \mathrm{kpc}^{-1}$. Peimbert, Torres-Peimbert, and Rayo (1978) mention that a fit to all five H II regions gives a nitrogen gradient of $d(\log N/H)/dr = -0.11\ \mathrm{kpc}^{-1}$. However, they point out that the results for S298 may be unreliable, because the ionizing star is losing mass which may be nitrogen rich.

There are investigations of possible abundance gradients in the Galaxy apart from optical studies of gaseous nebulae which provide a less direct comparison to the results presented in this section. Churchwell and Walmsley (1975) have examined the H109α surveys to look for a dependence of electron temperature on distance from the galactic center. They find a weak correlation in the sense that T_e decreases with decreasing galactocentric distance, and they attribute the decrease to an abundance gradient. More recently, Churchwell *et al.* (1977) have obtained recombination line observations of H II regions that confirm the result of Churchwell and Walmsley. Their model calculations require an increase in Z by a factor of 1.5 between 10 and 5 kpc and a decrease by a factor of 1.2 between 10 and 13 kpc, if the electron temperature gradient is to be explained. If, as Peimbert and Torres-Peimbert (1974) have suggested, oxygen can be used as representative of the heavy-element abundance Z, then the observations of Churchwell *et al.* imply a gradient $d(\log O/H)/dr \approx -0.03$ to $-0.04\ \mathrm{kpc}^{-1}$, in agreement with the results of this paper.

Mayor (1976) has determined the metallicity gradient in the solar neighborhood from an analysis of the kinematical and photometric properties of

600 dF stars and 600 dG–gK stars. He finds for all the stars $d(\log M/H)/dr = -0.05 \pm 0.01$ kpc^{-1} (where M stands for metals). Considering only the youngest stars gives a slightly steeper gradient, $d(\log M/H)/dr = 0.10 \pm 0.02$ kpc^{-1}.

Before this section on abundance gradients is concluded, mention should be made of the trends in the important line ratios which are known to vary across other spiral galaxies. It is not clear to what extent the observations of these galactic H II regions can shed light on line intensities from extragalactic H II regions, because the nebulae in this study are systematically different in size, density, and surface brightness from the extragalactic H II regions. Also, the spectra observed for extragalactic H II regions generally are integrated spectra. The line ratio [N II]/[S II] has already been discussed. The ratio [N II]/[O II] shows generally the same gradients as does N/O, which is not surprising since [N II]/[O II] $\approx N^+/O^+ = N/O$. Two effects complicate the use of [N II]/[O II] as an N/O abundance indicator, however. First, since λ3727 and λλ6548, 6583 are well separated in wavelength, the reddening correction is important. Second, the coefficient relating [N II]/[O II] and N/O is a function of T_e; at a constant N/O ratio, [N II]/[O II] decreases by roughly a factor of 2 for a temperature increase from 8000 to 12,000 K.

Two previous studies (Courtès, Louise, and Monnet 1969; Sivan 1976) have found radial gradients in the ratio [N II]/Hα in galactic H II regions. The interpretation of an [N II]/Hα gradient is not straightforward; electron temperature, ionization, and abundance all affect the line ratio, although abundance gradients seem to be the preferred explanation. The ratio [N II]/Hα has been plotted against galactocentric distance in Figure 8. Each point represents the average of all the observations for one nebula. The ratio [N II]/Hα seems to increase with decreasing R. The magnitude of the increase is similar to that observed by Sivan (1976) and is also similar to the magnitude of the N/H gradient. The simplest explanation is that the nitrogen gradient is the cause of the line intensity gradient.

It is important to stress that, even if radial gradients in [N II]/Hα derived from observations of H II regions result from abundance gradients, large [N II]/Hα ratios observed in some galactic nuclei (e.g., Burbidge and Burbidge 1962; Peimbert 1968) may very well represent a completely different phenomenon (Searle 1976). Searle has emphasized that the nuclear spectra observed by Burbidge and Burbidge, for example, represent a spectral discontinuity rather than an extrapolation of the trend seen in [N II]/Hα across some galactic disks.

The principal results of this section can be summarized as follows:

1. Any helium gradient that exists is small (≤ -0.01 kpc^{-1}).

2. The nitrogen gradient presented in this section is less steep than that found by Peimbert, Torres-Peimbert, and Rayo (1978) and Torres-Peimbert and Peimbert (1977). The oxygen gradient is also less steep than that found by Peimbert, Torres-Peimbert, and Rayo but agrees with oxygen gradients from planetary nebulae and with metallicity gradients from stars and radio observations of H II regions. The results from my sample should be more reliable than other results from H II regions because of the larger number of H II regions, the slightly longer baseline, and the uniformity of the distance determination.

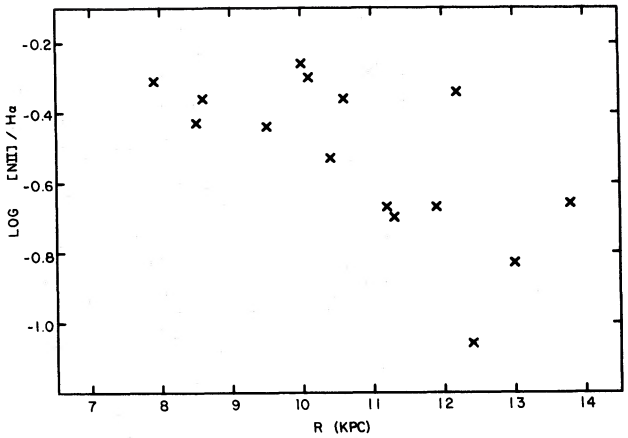

FIG. 8.—Observed line ratio [N II] λλ6548, 6583/Hα as a function of galactocentric distance for 15 galactic H II regions. The data are taken from Tables 1 and 3.

3. The line ratios [N II]/[S II], [N II]/[O II], and [N II]/Hα show gradients which, in the presence of the aforementioned abundance gradients, give further credence to the interpretation that line intensity gradients across other spiral galaxies result from abundance gradients. In this sample the line ratio [O III]/Hβ shows no correlation with galactocentric distance or derived oxygen abundance. Model calculations indicate that [O III]/Hβ does decrease with increasing oxygen abundance but that it decreases dramatically only for large oxygen overabundances (Shields 1974; Sarazin 1976; Hawley and Grandi 1977). Theories which use [O III]/Hβ as the sole indicator of heavy-element abundance (e.g., Jensen, Strom, and Strom 1976) are strongly dependent on assumptions concerning the ionization structure of H II regions.

VI. GRADIENTS IN M101

It would be desirable to compare the results for our Galaxy presented in § V to gradients in other spiral galaxies. Such a comparison is hampered by the unavailability of a complete set of line intensities; specifically lacking is [S III], and in many cases [O III] λ4363 or [N II] λ5755. The most complete set of data is that of Smith (1975) on M101, and in fewer than half of these H II regions was the electron temperature determined. Because [O III]/Hβ decreases systematically toward the nucleus, a temperature measurement necessarily relies on obtaining λ5755 of [N II]. I have therefore, as part of this investigation, reobserved two H II regions in M101 in order to obtain more accurate line intensities for the weak lines, which will

allow determination of abundance gradients not based solely on [N II]/[S II] gradients.

I have selected NGC 5455, which is at a projected distance of 13.6 kpc from the nucleus of M101 and has a high surface brightness, and Searle 5, which is at a projected distance of 6.9 kpc from the nucleus and is among the brightest of the inner-arm H II regions. The observations were obtained with the ITS and the Shane reflector in the manner described in § II. Since these H II regions have small apparent size, they were observed with one entrance aperture on the nebula and one on a suitable sky position.

The measured line intensities are presented in Table 7. The accuracy of these data is somewhat higher than quoted in § II because of the higher surface brightness of these extragalactic H II regions. The numbers in Table 7 result from 8 minutes of observing in both the "blue" and the "red" for NGC 5455, 8 minutes in the "blue" for Searle 5, and 48 minutes in the "red" for Searle 5. The intensity of [N II] λ6548 in NGC 5455 was taken to be $I(\lambda 6583)/3$. The intensities are in good agreement with the intensities of the lines which were also observed by Smith (1975).

The physical conditions and ionic abundances were computed in the manner described in § III. For NGC 5455, I derive $N_e = 300\ \mathrm{cm}^{-3}$ and $T_e([\mathrm{O\ III}]) = 10{,}200$ K. The difference between this value for T_e and Smith's result is due entirely to the different atomic constants. For Searle 5, $N_e \leq 100\ \mathrm{cm}^{-3}$. Unfortunately, even with an integration time of 48 minutes λ5755 was too faint to measure. The upper limit to $I(\lambda 5755)$ implies an upper limit to the electron temperature of 6950 K. For the purpose of calculating the ionic abundances, I have assumed $T_e = 6000$ K. Changing the electron temperature by 1000 K around 6000 K results in a change in the ionic abundances of a factor of from 2 to 3.

The total abundances were computed as described in § IV and are summarized in Table 8. I have included the He^+/H^+ ratios, because the correction to total helium abundance is uncertain, particularly in Searle 5 where the ionization is very low—$N(O)/N(O^{++}) = 18.3$. I have corrected the He^+/H^+ ratio in NGC 5455 by equation (6); but I have corrected the He^+/H^+ ratio in Searle 5 by $N(S)/[N(S) - N(S^+)]$, which is the next best approximation and is nearly correct since the ionization potential of S^+ is about the same as the ionization potential of He^0. Equation (6) gives a very different answer from $i_{cf} = N(S)/[N(S) - N(S^+)]$ and is surely suspect for regions of very low ionization.

The remarks made in § IV regarding the calculation of total abundances are applicable here. In particular, the neon abundance in Searle 5 is probably unreliable because of the low ionization. The total sulfur abundance in Searle 5 is not accurately determined, because [S III] λ6312 is very weak. The oxygen and nitrogen abundances are as accurate in these two H II regions as they are in the well-observed galactic H II regions.

I have included in Table 8 the emission line ratios which have been used by others as abundance diagnostics. In the final column of Table 8, I have listed

TABLE 7

LINE INTENSITIES IN H II REGIONS IN M101

		NGC 5455		SEARLE 5	
λ	ID	$F(\lambda)$	$I(\lambda)$	$F(\lambda)$	$I(\lambda)$
3727....	[O II]	179	208	157	222
3868....	[Ne III]	22.2	25.4	12.9	17.5
4071....	[S II]	3.0	3.3	7.2:	9.2:
4101....	Hδ	21.1	23.4	23.5	29.9
4340....	Hγ	41.1	44.5	41.1	49.2
4363....	[O III]	2.5	2.7	...	...
4861....	Hβ	100	100	100	100
4922....	He I	...	...	2.2	2.2
4959....	[O III]	125	123	7.4	7.2
5007....	[O III]	387	380	24.2	23.3
5755....	[N II]	...	...	< 0.6	< 0.5
5876....	He I	13.7	12.2	11.0	8.8
6312....	[S III]	1.6	1.4	0.4:	0.3:
6548....	[N II]	(11.4)	(9.6)	43.7	31.3
6563....	Hα	342	287	402	287
6583....	[N II]	34.2	28.7	131	93.3
6678....	He I	4.0	3.3	3.8	2.7
6717....	[S II]	20.6	17.1	43.9	30.7
6731....	[S II]	16.1	13.4	31.7	22.1

the ratios inner/outer for both abundances and line ratios. The ratio [N II]/[S II] increases by a factor of 1.9, while N/S increases by almost a factor of 5. This supports the conclusion of Hawley and Grandi (1977) that [N II]/[S II] is in some cases only a lower limit to the true N/S gradient. It seems that the changing oxygen abundance and possibly ionization have a large effect on [N II]/[S II]. The ratio [N II]/[O II] increases by slightly more than a factor of 3, while N/O actually seems to decrease, although, since the electron temperature of Searle 5 is unknown, the actual N/O ratio is also unknown. The increase in [N II]/[O II] is just what would be predicted with a constant N/O ratio and a temperature decrease (presumably due to an oxygen abundance increase) from 12,000 to 7000 K. The ratio [N II]/Hα increases and [O III]/Hβ decreases, as has been reported previously.

The abundances in Table 8 can be used to estimate gradients in M101. The baseline in galactocentric distance in M101 compares favorably with that for the H II regions in our Galaxy. Sivan (1976) gives values of the ratio of de Vaucouleurs and de Vaucouleurs (1964) for M101 and the Galaxy based on the equation of Freeman (1970). The ratio $R_0^{\mathrm{M101}}/R_0^{\mathrm{Galaxy}}$ is 1.28. Since this ratio is not much greater than unity, the resulting gradients (in kpc^{-1}) for M101 may be compared to gradients (in kpc^{-1}) for our Galaxy and the conclusions based on the comparison will not be very sensitive to whether the distances in the plane have been normalized.

To estimate the gradients in M101, I have simply taken the difference in abundance between Searle 5 and NGC 5455 divided by 6.7 kpc. As mentioned, the helium abundance in Searle 5 is uncertain. The gradient $d(\log \mathrm{He/H})/dr = +0.01\ \mathrm{kpc}^{-1}$ is consistent with my results for galactic H II regions. If one considers the uncertainties involved in correcting for the presence of neutral helium in H II regions, the data

TABLE 8

ABUNDANCES IN M101

Abundance Ratio	NGC 5455	Searle 5*	Inner/Outer
He^+/H^+	0.091	0.058	0.64
He/H	0.102	0.094	0.92
O/H	1.8×10^{-4}	1.1×10^{-3}	6.1
N/H	1.8×10^{-5}	9.8×10^{-5}	5.4
Ne/H	3.5×10^{-5}	4.5×10^{-3}	129
S/H	1.6×10^{-5}	1.8×10^{-5}	1.1
N/O	0.100	0.089	0.89
N/S	1.13	5.44:	4.8:
N^+/S^+	7.9	13.4	1.7
[O III]/Hβ	5.03	0.305	0.062
[N II]/[O II]	0.184	0.561	3.1
[N II]/[S II]	1.26	2.36	1.9
[N II]/Hα	0.133	0.434	3.3
(λ5876)/Hβ	0.122	0.088	0.72

* $T_e = 6000$ K was adopted.

presented here and in § V are consistent with there being no helium gradient in M101 or the Galaxy. The decrease in He^+ abundance shows that the ionization is lower in Searle 5 than in NGC 5455 [or, for the matter, in any of the H II regions in M101 for which Smith 1975 gives a value for $\eta = N(O)/N(O^{++})$]. Previous investigators have suggested that the stellar ionizing spectrum or dust content varies with abundance so as to produce a softer ionizing spectrum in the inner H II regions in spiral galaxies (Shields and Tinsley 1976; Sarazin 1976).

The oxygen gradient $d(\log O/H)/dr = -0.12\,\mathrm{kpc}^{-1}$ is steeper than the results for the galactic H II regions in my sample, while the nitrogen gradient $d(\log N/H)/dr = -0.11\,\mathrm{kpc}^{-1}$ agrees. It is difficult to quote uncertainties for the gradients in M101. The largest error must be introduced by the fact that these gradients are based on only two points. In addition, the electron temperature for the inner nebula has only been estimated. The gradient $d(\log N^+/S^+)/dr = -0.03\,\mathrm{kpc}^{-1}$ is less sensitive to the temperature and agrees with the results for our Galaxy.

Some measure of the uncertainty associated with these gradients may be obtained by estimating the same gradients using Smith's (1975) data alone. The H II regions with T_e determinations cover a total baseline of 4 kpc centered near 17 kpc from the nucleus. From the abundances in his Table 3, I compute $d(\log O/H)/dr = -0.05\,\mathrm{kpc}^{-1}$. As Smith noted, the N/O ratio appears to be constant, excluding NGC 5461. This would imply $d(\log N/H)/dr = -0.05\,\mathrm{kpc}^{-1}$. Including NGC 5461 yields $d(\log N/O)/dr \approx -0.02\,\mathrm{kpc}^{-1}$ and $d(\log N/H)/dr \approx -0.07\,\mathrm{kpc}^{-1}$. From the ratio [N II]/[S II], I compute $d(\log N^+/S^+)/dr = -0.02\,\mathrm{kpc}^{-1}$.

The various gradients for our Galaxy and for M101 are presented in Table 9. The results for M101 have been multiplied by 1.28 to correct for the different disk sizes. For Smith's $d(\log N/H)/dr$ and $d(\log N/O)/dr$, I have included the two values with and without NGC 5461. The difference between the results based on Smith's data and the results of this paper could be symptomatic of the uncertainty in determining these gradients, particularly when one considers the small number of H II regions involved. Alternatively, there could be evidence for steeper gradients closer to the nucleus. As is usually the case, more detailed observations are required.

TABLE 9

COMPARATIVE GRADIENTS*

Source	$\frac{d(\log He/H)}{dr}$	$\frac{d(\log O/H)}{dr}$	$\frac{d(\log N/H)}{dr}$	$\frac{d(\log N/O)}{dr}$	$\frac{d(\log N^+/S^+)}{dr}$
The Galaxy:					
This paper	0.00 ± 0.02	-0.04 ± 0.03	-0.10 ± 0.02	-0.06 ± 0.02	-0.05 ± 0.02
Peimbert *et al.* 1978 (H II regions)	-0.02 ± 0.01	-0.13 ± 0.04	-0.23 ± 0.04	~ -0.10	-0.09 ± 0.05
Torres-Peimbert and Peimbert (planetary nebulae)	-0.02 ± 0.01	-0.06 ± 0.02	-0.18 ± 0.04	...	...
Sivan (H II regions)	...	...	...	...	−0.04
M101:					
This paper	+0.01	−0.15	−0.14	+0.01	−0.04
Smith's data	...	−0.06	−0.05, −0.09†	0.00, −0.03†	−0.03

* Per kiloparsec.

† With NGC 5461.

Finally, there is evidence that the sulfur gradient in M101 is weaker than the oxygen gradient. The sulfur abundance in Searle 5 is uncertain because of the weakness of λ6312 and the unknown T_e, but it is unlikely that these errors are sufficient to account for the factor of more than 5 necessary to make the sulfur and oxygen gradients agree.

In summary, several points can be made concerning abundance gradients in M101 compared to the Galaxy. The oxygen gradients are not convincingly different at the level to which they are currently known. There is no significant difference in the N/H gradient between M101 and the galactic H II regions in my sample, although, from the N/O gradients, there may be some evidence for a steeper nitrogen gradient in the Galaxy compared to M101. There is not much indication of a gradient in N/O in M101. The gradients in N^+/S^+ appear to be the same; but this may not be very informative if, as Hawley and Grandi (1977) suggested, the N^+/S^+ gradient sets only a lower bound on the N/S gradients. One might expect a steeper nitrogen gradient in the Galaxy if metal gradients correlate with the mass of gas relative to total mass (Smith 1975). Presumably, a galaxy with less gas would have produced more stars and hence more heavy elements. The Galaxy has a smaller ratio M_{HI}/M_{total} than does M101 (Osterbrock 1974; Smith 1975) and has a hint of a steeper nitrogen gradient.

Finally, to the extent that NGC 5455 and Searle 5 represent extremes in abundance in M101, the results presented in Table 8 show that the magnitudes of the average abundances of oxygen, nitrogen, and sulfur are generally the same in M101 as in the Galaxy.

VII. SUMMARY

The principal results of this investigation can be summarized as follows:

1. There exist abundance gradients in oxygen and nitrogen among H II regions in the Galaxy. The magnitudes of these gradients are difficult to determine accurately, but they seem to be in agreement with gradients inferred from radio observations or observed in objects which are not extreme Population I.

2. There is no evidence in these data for a helium abundance difference between galactic H II regions and planetary nebulae, although such a difference could exist and go undetected if it were small (say, 10%). The correction for neutral helium is the primary uncertainty in the total helium abundance.

3. The average abundances of these 13 H II regions agree well with previously published results for the Orion Nebula.

4. Certain line ratios (e.g., [N II]/[S II] and [N II]/Hα) show generally the same gradients in the Galaxy as in other spiral galaxies. This supports the interpretation that line intensity gradients across other galaxies result from abundance gradients.

5. Abundance gradients in M101 are similar to abundance gradients in the Galaxy, although there is some evidence for a slightly steeper nitrogen gradient in the Galaxy. The magnitudes of the abundances are probably similar as well.

I am grateful to Drs. William G. Mathews, Donald E. Osterbrock, Patrick S. Osmer, and Leonard Searle for reading and commenting on the manuscript. I am grateful to Drs. Peimbert and Torres-Peimbert for a preprint of their paper on galactic H II regions. I had many interesting and useful conversations with Drs. Steven A. Grandi and Mark M. Phillips. Finally, it is a pleasure to thank my thesis adviser Dr. Joseph S. Miller for guidance and for the donations of 3 m observing time which made this project possible.

REFERENCES

Aller, L. 1976, *Pub. A.S.P.*, **88**, 574.
Balick, B., and Sneden, C. 1976, *Ap. J.*, **208**, 336.
Barker, T. 1978, *Ap. J.*, **220**, 193.
Benvenuti, P., D'Odorico, S., and Peimbert, M. 1973, *Astr. Ap.*, **28**, 447.
Brocklehurst, M. 1971, *M.N.R.A.S.*, **153**, 471.
———. 1972, *M.N.R.A.S.*, **157**, 211.
Burbidge, E. M., and Burbidge, G. R. 1962, *Ap. J.*, **135**, 694.
Churchwell, E., Smith, L. F., Mathis, J., and Mezger, P. G. 1977, preprint.
Churchwell, E., and Walmsley, C. M. 1975, *Astr. Ap.*, **38**, 451.
Comte, G. 1975, *Astr. Ap.*, **39**, 197.
Courtès, G., Louise, R., and Monnet, G. 1969, *Astr. Ap.*, **3**, 222.
de Vaucouleurs, G., and de Vaucouleurs, A. 1964, *Reference Catalogue of Bright Galaxies* (Austin: University of Texas Press).
D'Odorico, S., Peimbert, M., and Sabbadin, F. 1976, *Astr. Ap.*, **47**, 341.
Eissner, W., and Seaton, M. J. 1974, *J. Phys. B*, **7**, 2533.
Freeman, K. C. 1970, *Ap. J.*, **160**, 811.
Grandi, S. A. 1975, Ph.D. thesis, University of Arizona.
———. 1976, *Ap. J.*, **206**, 658.
Grandi, S. A., and Hawley, S. A. 1978, *Pub. A.S.P.*, **90**, 125.
Hawley, S. A., and Grandi, S. A. 1977, *Ap. J.*, **217**, 420.
Hawley, S. A., and Miller, J. S. 1977, *Ap. J.*, **212**, 94.
———. 1978, *Pub. A.S.P.*, **90**, 39.
Hayes, D. S. 1970, *Ap. J.*, **159**, 165.
Hayes, D. S., and Latham, D. W. 1975, *Ap. J.*, **197**, 593.
Jensen, E. B., Strom, K. M., and Strom, S. E. 1976, *Ap. J.*, **209**, 748.
Lee, T. A. 1968, *Ap. J.*, **152**, 913.
Mayor, M. 1976, *Astr. Ap.*, **48**, 301.
Mihalas, D. 1972, *Non-LTE Model Atmospheres for B and O Stars* (NCAR Tech. Note, No. STR-76).
Miller, J. S. 1968, *Ap. J.*, **151**, 473.
Miller, J. S., and Mathews, W. G. 1972, *Ap. J.*, **172**, 593.
Miller, J. S., Robinson, L. B., and Wampler, E. J. 1976, *Advances in Electronics and Electron Physics* (New York: Academic Press).
Osterbrock, D. E. 1974, *Astrophysics of Gaseous Nebula* (San Francisco: Freeman).
Peimbert, M. 1967, *Ap. J.*, **150**, 825.
———. 1968, *Ap. J.*, **154**, 33.
Peimbert, M., and Costero, R. 1969, *Bol. Obs. Tonantzintla y Tacubaya*, **5**, 3.
Peimbert, M., Rodriquez, L., and Torres-Peimbert, S. 1974, *Revista Mexicana Astr. Ap.*, **1**, 129.
Peimbert, M., and Torres-Peimbert, S. 1971, *Ap. J.*, **168**, 413.
———. 1974, *Ap. J.*, **193**, 327.
———. 1976, *Ap. J.*, **203**, 581.
———. 1977, *M.N.R.A.S.*, **179**, 217.
Peimbert, M., Torres-Peimbert, S., and Rayo, J. F. 1978, *Ap. J.*, **220**, 516.
Pradhan, A. K. 1974, *J. Phys. B*, **7**, L105.

Robinson, L. B., and Wampler, E. J. 1972, *Pub. A.S.P.*, **84**, 161.
Sarazin, C. L. 1976, *Ap. J.*, **208**, 323.
Searle, C. L. 1971, *Ap. J.*, **168**, 327.
Searle, L. 1976, *Royal Obs. Bull.*, No. 182, p. 119.
Searle, L., and Sargent, W. L. W. 1972, *Ap. J.*, **173**, 25.
Seaton, M. J. 1975, *M.N.R.A.S.*, **170**, 475.
Shields, G. A. 1974, *Ap. J.*, **193**, 335.
Shields, G. A., and Tinsley, B. M. 1976, *Ap. J.*, **203**, 66.
Sivan, J. P. 1976, *Astr. Ap.*, **49**, 173.
Smith, H. E. 1975, *Ap. J.*, **199**, 591.
Stone, R. P. S. 1977, *Ap. J.*, **218**, 767.
Torres-Peimbert, S., and Peimbert, M. 1971, *Bol. Obs. Tonantzintla y Tacubaya*, **6**, 101.
———. 1977, preprint.
Wampler, E. J. 1966, *Ap. J.*, **144**, 921.
Whitford, A. E. 1958, *A.J.*, **63**, 201.

STEVEN A. HAWLEY: Cerro Tololo Inter-American Observatory, Casilla 63-D, La Serena, Chile